Modeling Membrane Filtration of Protein and Cell Suspensions in a Vortex Flow Filtration System

M. Mateus and J. M. S. Cabral
Laboratório de Engenharia Bioquímica, Instituto Superior Técnico, Av. Rovisco Pais, 1000 Lisboa, Portugal

Vortex flow filtration experiments with bovine serum albumin (BSA) solutions and Arthrobacter simplex cell suspensions in a rotary membrane device are modeled in the pressure-dependent flux and mass-transfer-controlled regions. An expression for the concentration-dependent diffusion coefficients accounting for hydrodynamic and long-range potential interactions between rigid spherical macromolecules is used for BSA. A shear-induced diffusion coefficient, strongly concentration-dependent on the cell concentration, is assumed to describe the diffusion behavior of the cell suspensions. The adjusted model parameters for albumin solutions in the pressure-dependent region of flux predict the permeation flux behavior for A. simplex cell suspensions. When the mass-transfer correlation is calculated using cell diffusion coefficients, based on a volumetric cell fraction that is around half of the average value of the calculated membrane surface fractions, the fluxes are estimated within less than 10.5% relative error. In the mass-transfer-controlled region of flux, the volume fractions of cells at the membrane surface are between 0.16 and 0.35, depending on bulk concentration and hydrodynamic conditions.

Introduction

Membrane filtration is an important unit operation in the downstream processing of biological materials (Mateus et al., 1993), such as whole cells, proteins, and low molecular weight products. The most serious problems in membrane filtration are concentration polarization due to the formation of a gel layer and membrane fouling, which decrease the transmembrane flux rates and product recovery.

Several methods have been used to control concentration polarization and the associated membrane fouling. Vortex flow filtration (VFF) has been used (López-Leiva, 1979; Holeschovsky and Cooney, 1991; Mateus and Cabral, 1991) as a process leading to the improved performance of membrane filtration. Taylor vortices are promoted on the membrane filtration surface by rotation, preventing the formation of the gel layer. The theory of VFF has been reported and a few mathematical models developed to interpret the data of protein model systems (López-Leiva, 1979; Holeschovsky and Cooney, 1991).

Steroids have been produced by biotransformation, and their recovery can be accomplished by membrane filtration (Mateus and Cabral, 1989, 1991), as an example of the application of membrane processes to the primary isolation of low molecular weight biological products.

This article describes the VFF of steroids (6α-methylprednisolone) from biotransformation media in the presence and absence of cells (*Arthrobacter simplex*) at different rotation speeds. Bovine serum albumin (BSA) was added to the cell-free biotransformation media as a concentration polarization promoter.

Mathematical Models

In this article two different models, the resistances in series and the mass-transfer model, are studied in different regimes of permeation flux and combined to describe the same phenomena. Although both of these models can be used in all ranges of operating pressures, in this article the model of the resistances in series is applied to the lower operating pressure range, while the mass-transfer model is applied to the higher pressure range.

Model of resistances in series

In the pressure-dependent region, when flux is controlled both by the membrane and the boundary-layer resistances,

Correspondence concerning this article should be addressed to J. M. S. Cabral.

the model of resistances in series can be applied, and the permeation flux through the membrane is described by the equation,

$$J = (\Delta P - \Delta\pi)/[(1/k_m) + (1/k_1)]. \quad (1)$$

Using the π-theorem of dimensional analysis, the Sherwood number defined for mass transfer through the boundary layer in this transition region, $Sh = k_1(d_h/D)\,(\Delta P - \Delta\pi)$, is given by

$$Sh = f_1\left(Re_a, Ta, Sc, \left[(\Delta P - \Delta\pi)(Rd^3)^{1/2}/(\rho\nu^2)\right], \sigma, C_b/\rho\right). \quad (2)$$

In systems where the osmotic pressure was negligible, this function was found to be (López-Leiva, 1979)

$$k_1(d_h/D)\,\Delta P = 0.34\,Ta^{2.43}\left[\Delta P\,(Rd^3)^{1/2}/(\rho\nu^2)\right]^{-1.15} Sc^{1/3}. \quad (3)$$

Mass-transfer model

The flux in the mass-transfer-controlled region is described by Eq. 4 as the result of a mass balance on a differential element, at steady state:

$$JC = JC_f + D\,\partial C/\partial x. \quad (4)$$

This equation states that the convective flux of the solute (or particles) that reaches the membrane surface is equal to the sum of solute leakage to the permeate and diffusive transport of solute back to the bulk fluid. When the membrane completely retains the solute (or particle), the solute concentration in the permeate equals zero ($C_f = 0$) and the second term in Eq. 4 simplifies to the diffusive part.

If the diffusion coefficient is itself a function of solute concentration (Eq. 5), which is the real situation for proteins and other charged macromolecules at finite concentrations,

$$D = D^0(1 + bC), \quad (5)$$

the flux, upon integration in x, from the bulk flow to the membrane layer is given by

$$J = k[(1 + bC_f)\ln|(C_l - C_f)/(C_b - C_f)| + b(C_l - C_b)], \quad (6)$$

where $D^0/\delta = k$ is the mass-transfer coefficient, computed for bulk flow conditions in our study. When the diffusion coefficient is constant ($b = 0$) and the membrane is totally retentive, Eq. 6 describes the mass transfer model (Michaels, 1968).

For electrically charged macromolecules, such as proteins, the value of the parameter b can be estimated with reasonable accuracy. The first-order volume fraction dependence of the macroscopic diffusion coefficient may be obtained by combining the migration and stochastic contributions to molecular transport,

$$D/D^0 = 1 + [8(\mathrm{I} - \Lambda)]\phi, \quad (7)$$

where I represents the effect of direct long-range forces between particles on the movement of a test particle placed in a macroscopic concentration gradient, and Λ is a correction to the Stokes-Einstein equation for Brownian diffusion and accounts for hydrodynamic interactions between particles. Both I and Λ are complex integrals of the long-range intermolecule potential energy; they have been numerically computed (Anderson and Reed, 1976). Therefore, I and Λ are functions of the molecule diameter, ionic strength of the solvent (pI) and charge of the molecule, which depends on the pH and also on the pI of the solvent (Anderson and Reed, 1976).

In tangential flow membrane microfiltration, the large difference (by one to two orders of magnitude) between the experimental permeation fluxes and the lower values predicted by the mass-transfer model is commonly known as "the flux paradox for colloidal particles." In the mass-transfer model, the molecular diffusivity is calculated by the Stokes-Einstein relation, based on the Brownian motion of particles. For the particles involved in microfiltration processes (MF), with diameters much larger than molecular diameters, the Brownian motion is negligible (Lojkine et al., 1992). Therefore, the enhanced back diffusion in MF must be due to some other phenomenon. Induced by shear flow, the particles self-diffuse and are characterized by a self-diffusion coefficient that is a strong function of particle concentration (Eckstein et al., 1977; Leighton and Acrivos, 1987a). In the presence of a concentration gradient, such as the one due to a concentration polarization phenomenon, local gradients in viscosity are generated. Both gradients induce a drift of particles from regions of high to low concentration. The total effective diffusivity is due to this particle drift in addition to that provided by random self-diffusion. This diffusivity was correlated as a function of particle concentration for both diffusions normal to the plane and within the plane of shear. The last situation was only described for $0.4 \le \phi \le 0.5$ (Leighton and Acrivos, 1987b). The effective diffusivity in the plane of shear was extended to the lower values of ϕ by combining these results with those for the random self-diffusion of particles (Leighton and Acrivos, 1986), giving

$$D \approx 0.33\,\gamma_m\, r_p^2\,\phi^2[1 + 0.5\exp(8.8\,\phi)]. \quad (8)$$

Hence, making use of this coefficient of shear-induced diffusion, the flux of the solvent is given by Eq. 9, upon integration of Eq. 4, for the case of filtration of cell suspensions with a totally retentive ultrafiltration membrane ($C_f = 0$):

$$J = \left(0.33\,\gamma_m\, r_p^2/\delta\right)\{0.5(\phi_1^2 - \phi_b^2) + 0.5[\exp(8.8\,\phi_1)(\phi_1/8.8 - 1/8.8^2) - \exp(8.8\,\phi_b)(\phi_b/8.8 - 1/8.8^2)]\}. \quad (9)$$

In accordance with Eq. 8, the following relation can be written:

$$0.33\,\gamma_m\,r_p^2 \approx D_b/\{\phi_b^2[1+0.5\exp(8.8\,\phi_b)]\}. \quad (10)$$

One possible solution to the equation of flux is

$$J = k\{0.5(\phi_1^2 - \phi_b^2) + 0.5[\exp(8.8\,\phi_1)(\phi_1/8.8 - 1/8.8^2) - \exp(8.8\,\phi_b)(\phi_b/8.8 - 1/8.8^2)]\}/\{\phi_b^2[1+0.5\exp(8.8\,\phi_b)]\}, \quad (11)$$

where $D_b/\delta = k$ is the mass-transfer coefficient, computed at bulk fluid conditions.

The mass-transfer coefficient in rotary membrane systems can be correlated by the following dimensionless expression, obtained by analogy with the heat-transfer phenomenon (López-Leiva, 1979),

$$k_{II}\,d_h/D = f_{II}(Re_a, Ta, Sc) \quad (12)$$

or by another expression (Holeschovsky and Cooney, 1991), which also correlates to the rotary module design

$$k_{III}\,d_h/D = f_{III}(Re_a, Ta, d_h/R, Sc). \quad (13)$$

These authors, using a rotary module from the same manufacturer as the one used in this article, obtained Eq. 14 for the Sherwood number, with a 2.2 percent standard deviation:

$$Sh = 1.26\,Ta^{0.5}(2d/R)^{0.17}\,Sc^{0.33}. \quad (14)$$

Experimental Apparatus and Procedure

Ultrafiltration system

Ultrafiltration experiments were carried out on simulated steroid biotransformation media: the corticosteroid 6α-methylprednisolone (0.30 g/L) was solubilized in the solvent—26 mM phosphate buffer, pH 7.3, containing 2.5% (v/v) methanol. We added a model protein, BSA, to the final concentrations of 0.10, 1.0 and 10 g/L of this solution, or we added freeze-dried *A. simplex* cells to the final concentrations of 1.5, 3.0 and 15 g (60°C d.w.)/L. After thermostabilization at 30°C, the solution/suspension was fed into a 0.020-m^2 100,000-MWCO (molecular weight cutoff) polyacrylonitrile rotary membrane system (Benchmark, from Membrex, Inc.) at the lowest pressure (6–7 psi, 41–48 kPa) of study, with total recirculation of the permeate and retentate. After steady-state flux was reached, other pressures were then input.

As this system only incorporates one pressure transducer, at the retentate outlet, the pressure readings were corrected for centrifugal pressure effects at the different rotation speeds by plotting water ultrafiltration fluxes of permeate against retentate outlet pressure readings. The corrections imposed zero permeation flux at zero transmembrane pressure (Figure 1).

Arthrobacter simplex cell suspensions

A. simplex ATCC 6946 cells were grown on a medium of yeast extract (10 g/L), K_2HPO_4 (3 g/L), and KH_2PO_4 (1 g/L).

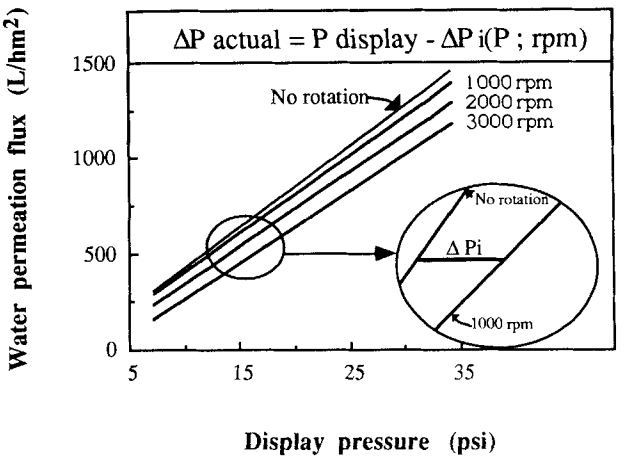

Figure 1. Corrections made on the display pressure for calculation of the average transmembrane pressure.

In an early exponential phase (0.7 optical density) the cells were induced for $\Delta^{1,2}$-dehydrogenase activity with the addition of 0.5 g/L hydrocortisone. The fermentation was run in a 20-L fermenter at 30°C and pH 7.3 for 21 h, until a final concentration of 2 g (60°C d.w.)/L was reached at the beginning of the stationary growth phase. Then cells were harvested by centrifugation and freeze-dried for further use.

A 3.0-g-d.w./L cell suspension was diluted (1:2,000–1:5,000) with a buffer/methanol solution and cell counts [$(1.9 \pm 0.4) \times 10^{10}$ cells/mL] were done in a hemocytometer. For volume fraction calculations, this suspension was assumed to have 2×10^{10} cells/mL. The *A. simplex* cells in the exponential growth phase are irregular rods 0.5–0.9 μm $\times$ 1.0–4.0 μm. A volume-based (50% prolates and oblates) average cell radius was calculated as an equivalent radius of a sphere, r_p of 0.68 μm. Then, the concentrations of cell suspensions used in this work and expressed as volume fractions were 0.0147, 0.0293, and 0.147.

Operating parameters

In this article the recirculating flow rate was kept constant at 500 mL/min. Fluid densities and viscosities (Brookfield LVTDV-II cP viscosimeter) of protein solutions and cell suspensions were measured. Due to the low concentrations used, these values differed slightly from water values. Therefore, small changes in the axial Reynolds number were obtained for runs of different solution/suspension composition. However, there is evidence that the axial Reynolds number has no influence on the permeation fluxes in rotary systems (Holeschovsky and Cooney, 1991) within the operating conditions of the experiments (Table 1).

Calculations

BSA diffusion coefficient

For the diffusivity of BSA in the described solvent, the b parameter in Eq. 5 was estimated to be 0.0101. Although several assumptions had to be made (see Table 2), this value is a

Table 1. Bulk Flow Operating Parameters at 30°C in the Rotary Membrane Filtration Runs, Expressed as Dimensionless Numbers

Process fluid	Parameter	Range of values
BSA solutions	Re (axial)	114–128
	Re (tangential)	9,100–20,400
	Ta	1,300–3,000
	Sc*	15,500–16,000
A. simplex suspensions	Re (axial)	96–123
	Re (tangential)	7,700–19,700
	Ta	1,100–2,900
	Sc**	4,900–2,700,000

*Diffusivities according to Eq. 15.
**Diffusivities according to Eq. 8. For cell concentrations of 1.5 g/L and 3.0 g/L at 1000 rpm the Stokes-Einstein law for Brownian motion was used since shear-induced diffusion was meaningless compared to this.

good approximation, according to the Anderson and Reed theoretical work to which experimental work has given support (Fair et al., 1978). Converting the diffusivity at infinite dilution for 30°C, Eq. 15 was obtained for BSA diffusivity:

$$D\ (\mathrm{m^2/s}) = 5.81\times10^{-11}[1+0.0101C\ (\mathrm{g/L})]. \qquad (15)$$

Curve fittings

The model parameters were iterated—using the Solver Function facility of the Microsoft-Excel Windows application—to obtain the best description of the experimental values (minimum of the sum of the module of relative errors, for all the runs, between experimental and calculated flux values). The iteration parameters are indicated below:

Cell-free Biotransformation Media. For the transition (pressure-dependent) region of flux, the membrane mass-transfer coefficients, the independent constant, and the exponents affecting the dimensionless numbers were iterated. The exponent of the Schmidt number was assumed to be 1/3.

Table 2 Characteristic Parameters for BSA in Solution Used to Determine Parameter *b* in Eq. 5

Parameter	Value	Reference
Diffusion coefficient at infinite dilution for 21.5°C (m^2/s)	5.66×10^{-11}	Fair et al., 1978
Molecular weight (dalton)	66,500	Freifelder, 1982
Charge*(e.u.)	−15	—
Partial molar volume (L/kg)	0.736	Hinz, 1986
Molecular radius (Å)	36	Anderson and Reed, 1976
Debye length (Å)**	13.5	Moore, 1962; Kirkwood and Shumaker, 1952

*Value calculated at pH 7.3, with the CHARGPRO program that is based in the primary structure of the protein and assumes that no three-dimensional structures interfere with ionization states (database of PC/GENE actualized to Aug. 1992).
**This calculation does not account for the contributions of the fluctuating charges of the proteins.

For the mass-transfer controlled region of flux, the Holeschovsky and Cooney correlation was used in the calculation of the mass-transfer coefficient. Protein concentrations at the membrane surface were calculated for each steady state dependent on BSA permeate concentration.

A. Simplex Biotransformation Media. The parameters adjusted for BSA experiments in the transition region of flux were used in the filtration modeling of the *A. simplex* suspensions. The values of the membrane mass-transfer coefficient were adapted from the BSA experiments, according to changes in fluid viscosity and the Hagen-Poiseuille law.

The Holeschovsky and Cooney's correlation was also used in the mass-transfer-controlled region of flux. The diffusion coefficient used was the one described by a shear-induced migration of particles (Eq. 8). The cell volume fraction at the membrane surface was the iteration parameter.

Results and Discussion

Permeation experiments

Permeation fluxes and observed protein rejections for BSA runs and permeation fluxes for *A. simplex* runs are depicted in Figures 2 and 3 , respectively. The experiments when the membrane was steady are also included, as they are elucidative of some events, though they were not correlated. When the membrane is not rotating, the boundary layer control becomes dependent on the axial Reynolds number and the fluid regime is laminar. Since Re_a at the entrance of the module

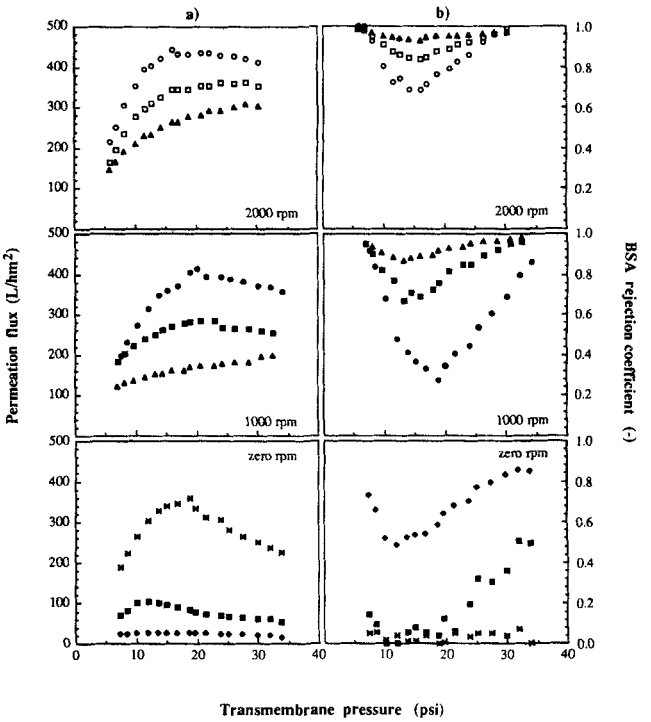

Figure 2. Vortex flow filtration of cell-free biotransformation media (BSA experiments).

Permeation flux (a) and BSA rejection coefficient (b), as a function of the transmembrane pressure. Legend: BSA bulk concentrations of ○ ● × — 0.10 g/L; □ ■ ⊞ —1.0 g/L; and △ ▲ ◇ — 10 g/L.

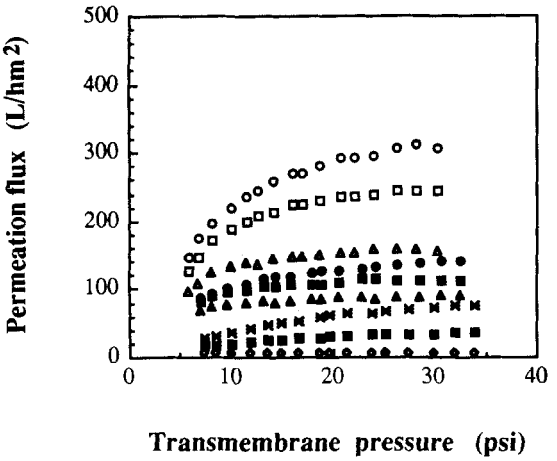

Figure 3. Vortex flow filtration of *A. simplex* biotransformation media.

Permeation flux as a function of the transmembrane pressure. Legend: *A. simplex* bulk concentrations of ○ ● ×—1.5 g/L; □ ■ ⊞—3.0 g/L; and △ ▲ ◇— 15 g/L; open symbols—2,000 rpm; black symbols—1,000 rpm; other symbols—0 rpm.

was kept at low values, it was variable along the axis of the annulus due to the permeation flux, and an axial analysis has to be applied. Steroid rejection coefficients in these experiments are shown in Table 3. From these results, three major comments can be made:

(1) The filtration runs of albumin show a flux decrease pattern at higher transmembrane pressures and lower bulk concentrations that filtration of cell suspensions does not present. The flux decay becomes more pronounced, the lower the rotation speed of the membrane, which could be attributed to a greater capability of compacting the thicker membrane filtration boundary layers, and the less concentrated the solution. This fact is probably due to the effect of pressure on the adsorption of proteins on the membrane surface. A greater effect would be at the surface where there are more free binding sites.

(2) The effect of shear is more important in the filtration of cell suspensions than in the filtration of protein solutions. This behavior is consistent with the hypothesis of the shear-dependent back-diffusion of particles.

(3) The permeation fluxes are not controlled by the steroid in the filtration broths, as its rejection by the membrane is very low. Nevertheless, a small amount of steroid leaves the bulk solution to be retained in the polarization layer during the filtration (≈ 0–10%, depending on the bulk concentrations of BSA or cells and hydrodynamic conditions of each run). With this filtration system at zero rotation speed, there is no adsorption of the steroid after 7 h of total recirculation of steroid/buffer/methanol solutions, even at a transmembrane pressure of 34 psi (234 kPa). Also there is no change in the membrane permeability due to the presence of the steroid. This can be attributed to the high hydrophilicity of the Membrex polyacrylonitrile membrane (Mateus and Cabral, 1991).

Modeling of the permeation flux in the transition region

Neglecting the osmotic pressure, the best fit of the experimental values is obtained when the flux is described by Eq. 1

Table 3. Average Rejection Coefficient for the Steroid 6α-Methylprednisolone within the Average Transmembrane Pressures Tested at Different BSA and *A. simplex* Cell Concentrations

Rotation Speed (rpm)	Conc. of BSA in Bulk Flow (g/L)		
	0.100	1.00	10.0
0	0.000	0.000	0.092 ± 0.018
1,000	0.008 ± 0.006	0.027 ± 0.011	0.121 ± 0.011
2,000	0.009 ± 0.007	0.023 ± 0.011	0.119 ± 0.012
	Conc. of *A. Simplex* Cells in Bulk Flow (g/L)		
	1.50	3.00	15.0
0	0.000	0.000	0.078 ± 0.026
1,000	0.000	0.041 ± 0.011	0.169 ± 0.012
2,000	0.000	0.042 ± 0.011	0.145 ± 0.013

and the correlation for the Sherwood number [$Sh = k_1(d_h/D)\Delta P$] is the following:

$$Sh = 0.42\,Ta^{1.24}\left[\Delta P\,(Rd^3)^{1/2}/(\rho\nu^2)\right]^{-0.25} Sc^{1/3}\,(C_b/\rho).^{-0.38} \tag{16}$$

The flux is calculated with an average relative error of 5.0% and none of the calculations deviates more than 8.6% from the experimental value. A fifth exponent of C_b/ρ had to be added to the correlation of López-Leiva, or the error would increase to 20% (with new adjusts to the other exponents). A plot of calculated and experimental values of permeation flux for cell-free biotransformation media is presented in Figure 4.

Using the López-Leiva correlation, the fluxes are 100% underpredicted. This correlation largely underpredicts the mass-transfer coefficient. As was already mentioned, it is unlikely that the axial Reynolds number not considered in the correlation could account for these differences. López-Leiva verified that at least a Re_a of 150 was needed for a flux inde-

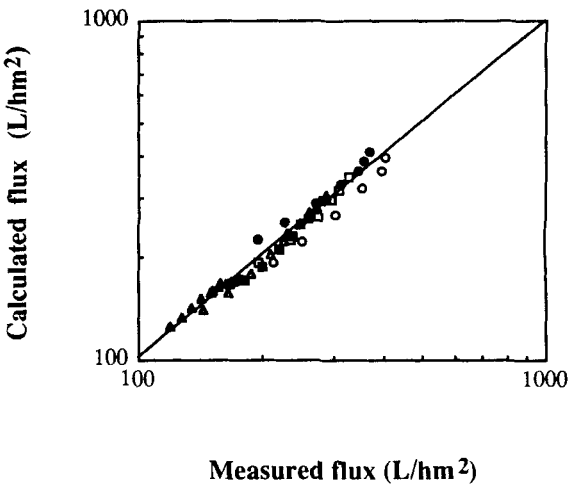

Figure 4. Permeation flux for cell-free biotransformation media in the pressure-dependent region at 1,000 and 2,000 rpm, according to Eq. 16.

Legends as in Figure 2.

pendent of an axial Reynolds number. According to his results for the values used in this work the decay in flux would be around 0.5%. Kataoka et al. (1977) studied mass transfer in these annular flow systems and showed that average Sherwood numbers decrease with increasing Reynolds number as long as Taylor vortices exist and that the value of the Sherwood number (up to a Re_a of 50) can be 30–50% of the value at a zero axial flow rate. Therefore, the unaccounted-for axial Reynolds number does not explain the 100% error in flux prediction.

The estimated membrane mass-transfer coefficients were 34.8, 31.9, and 29.4 L/hm^2 · psi for BSA concentrations of 0.100, 1.00, and 10.0 g/L, respectively. These values are close to the ones expected if the k_m value at the lower BSA concentration is assumed to be equal to the solvent permeability (33.0 L/hm^2 · psi). At the other BSA concentrations, the predicted k_m values are 31.7 and 29.5 L/hm^2 · psi, respectively. These values were obtained by correction of the solvent permeability, taking into account the different fluid viscosities and the Hagen-Poiseuille law. However, in the development of the model by López-Leiva, the membrane permeability is assumed to be dependent on bulk flow concentration, being always lower than membrane permeability due to a monomolecular layer of protein adsorbed to the membrane (López-Leiva, 1979).

With BSA solutions, the flux obtained in the Membrex system is much less dependent on the Taylor number (power number of 1.24, instead of 2.43) and pressure (power number of −1.25, instead of −2.15) than the one verified by López-Leiva with a DDS 600 membrane in a rotary system. Probably the low BSA adsorption characteristics (high hydrophilicity) of this polyacrylonitrile membrane (Rolchigo et al., 1989) are responsible for this lower dependence.

Characterization of the boundary layer mass transfer has been frequently reported based on the bulk flow conditions. The use of Eq. 16 to describe the mass transfer in vortex flow filtration of *A. simplex* suspensions failed when the bulk flow variables were used. The fluxes were always underpredicted. One explanation can be made based on the fact that most of the work done so far has been looking at the transfer of molecules for which the dependence of diffusivity on its concentration is weak. However, the strongly concentration-dependent shear-induced diffusivity (Eq. 8) has to be taken into account for the filtration of cell suspensions. Hence, while using bulk flow conditions for other fluid variables than diffusivity makes no difference, for this one boundary layer conditions should be considered.

Calculated and experimental permeation fluxes of *A. simplex* biotransformation media at 1,000 and 2,000 rpm are presented in Figure 5. It can be seen that larger deviations occur at 1,000 rpm. According to the work of Kataoka et al. (1977), it can be estimated that the flow regimes are different at these two rotation speeds: stable laminar vortex flow with no secondary vortices and laminar vortex flow with secondary vortices near the inner rotating cylinder (a transition state to the turbulent vortex flow), at 1,000 and 2,000 rpm, respectively.

The different flow regimes could be responsible for the deviations. This model does not account for the physical characteristics of the system (changes in packing of deposited solids associated with applied pressure or cell size or others). The larger deviations at 1,000 rpm seem to be related to a

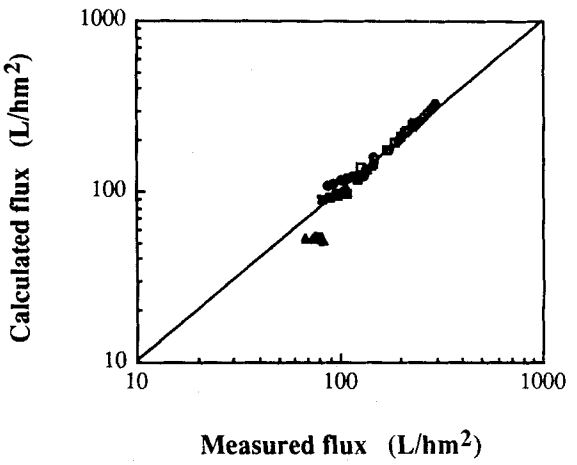

Figure 5. Permeation flux for *A. simplex* biotransformation media in the pressure-dependent region at 1,000 and 2,000 rpm, according to Eq. 16.

Legends as in Figure 3.

different pressure profile of deposited solids. In the pressure-dependent region of flux, a linear relation of ϕ with pressure between the bulk and the maximum membrane surface concentration (determined by the mass-transfer model) overpredicts the flux for all the runs. An exception was the run at 1,000 rpm for the higher bulk cell concentration. Nevertheless, in the deposition layer the linear concentration-pressure profile more closely described the behavior of the 1,000 rpm runs, while the runs at 2,000 rpm were well described by a flat concentration-pressure profile.

It seems that Eq. 16 is more adequate for the laminar vortex flow with the secondary vortices regime. The compaction behavior of the cell layer in this regime seems to be closer to that of BSA, the model compound used to predict the cell suspension behavior.

Modeling of the permeation flux in the mass-transfer controlled region

Equations 6 and 11, together with Eq. 14, were used to fit the experimental data of BSA and cell suspensions, respectively. The values obtained for the membrane surface concentrations are indicated in Figure 6 and Table 4.

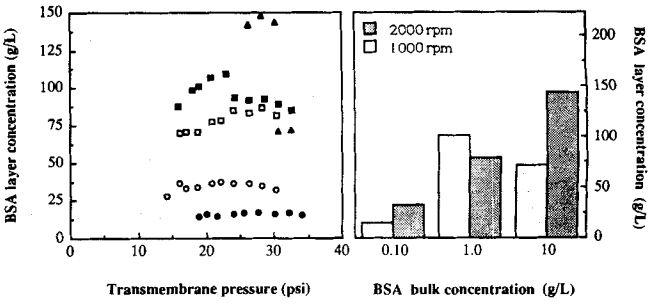

Figure 6. Estimated BSA layer concentrations at the membrane surface, as a function of transmembrane pressure and average values.

Legends as in Figure 2.

Table 4. Estimated Layer Concentrations of *A. simplex* Cells (Expressed in Volume Fractions), Using the Models Described for Mass-Transfer Control of Flux

Rotation Speed (rpm)	Conc. of *A. Simplex* in Bulk Flow (g/L)		
	1.50	3.00	15.0
1,000	0.16	0.25	0.34
2,000	0.21	0.28	0.35

For BSA experiments, the fittings were done at each pressure, and wall concentrations reflect the scatter of the experimental points. For the filtration of cell suspensions, the best estimated concentrations at the membrane surface for all pressure readings lead to calculated flux rates with an average relative error of 1.5%.

When the membrane is permeated by the solute, an increase in pressure leads to a slight increase in flux and a simultaneous increase in membrane surface concentration. Due to closer packing, the membrane becomes less permeable to the solute and protein rejection increases. As the pressure continues to increase, flux starts to decrease and rejection also increases, which suggests that the protein layer is compacting. It can also be seen that the predicted protein concentration at the membrane surface becomes lower at this stage. A misleading calculation might be responsible for this result, as boundary layer properties may have changed from the bulk flow conditions so that the mass-transfer coefficient could be lower than predicted and concentrations higher than estimated for those values of pressure.

The larger protein concentration at the membrane surface (147 g BSA/L) for this region of flux at higher transmembrane pressures (28 psi, 193 kPa) was verified at 2,000 rpm and 10 g BSA/L. An osmotic pressure of around 3 psi was raised in this BSA solution at pH 7.3 (Vilker et al., 1984); for the other runs, the osmotic pressure was negligible. Therefore, the simplification of the model of resistances in series at lower transmembrane pressures seems reasonable.

Predicted concentrations of cells at the membrane surface vary from 0.16 to 0.35 in volume fractions, which correspond to 16 to 36 g (60°C d.w.)/L. As in the BSA experiments, the concentration of cells on the membrane surface depends on the bulk flow concentrations and membrane rotation speed. At higher bulk flow concentrations, the adsorption on the membrane is higher and flux is lower, but by increasing the shear at the membrane surface, the membrane boundary layer can be favorably controlled and flux increased, leading to an even higher surface concentration, as a larger number of particles come to the membrane by convection. The enhancement in membrane surface concentration at increased rotation speed is less pronounced for higher cell concentrations. The reason may be the fewer adsorption sites.

Other authors (Zydney and Colton, 1986) also adapted a model of shear-induced diffusion of particles (by Eckstein) to the mass-transfer model, where the mass-transfer coefficient was described by the Lévèque correlation for the Sherwood number. Their main work on microfiltration of blood was also extended for bacterial suspensions and other nonblood experiments. Membrane concentrations of bacteria of 0.69 in volume fraction were reported for shear rates and bulk concentrations close to the ones used in this study. Their best fit for blood data has deviations of 30%, while for the nonblood experiments the deviations extend to 53%. These deviations are computed in a manner that for small differences between calculated and experimental flux values are equal to average relative errors. However, the authors did not sum the absolute values of the deviations, so negative contributions to the error will balance the positive values. Therefore, the real deviations can be higher than the ones indicated. In the present study much lower deviations (1.5%) were obtained. Although fewer data were correlated, the establishment of a membrane layer concentration independent of the hydrodynamic conditions of the experiment was not tried. The reason for the large difference in membrane layer concentrations when compared to Zydney and Colton's results is partially due to the use by these authors of a correlation for shear-induced diffusion of particles that underpredicts this coefficient (Leighton and Acrivos, 1987b).

It should be emphasized that the mass-transfer coefficient is reported with respect to the bulk flow characteristics when it should be reported with respect to the boundary layer conditions. Hence, mass-transfer coefficients may be higher than those calculated (boundary layer concentrations are higher and so are diffusivities), and actual membrane surface concentrations may be even lower than the ones indicated in Table 4.

The development of Eq. 11 implicitly assumed a constant shear rate across the boundary layer. Especially close to the membrane surface where higher cell concentrations exist the concentration gradient induces a viscosity gradient, and therefore the shear rate can decrease significantly from its value at bulk concentrations. The work presented here can be regarded as a simplification.

Romero and Davis (1988) and Davis and Sherwood (1990) developed a shear-induced diffusion model for TFF (also after Eq. 8) that was able to theoretically describe the permeation flux along the membrane length, solving differential mass balances that accounted for axial convection of particles and suspension viscosity dependence on particle volume fraction (empirically determined expression). These authors determined local nonlinear velocity profiles in the boundary layer. For most process situations, the permeation flux calculation involved numerical computation of integrals. The model of Davis and Sherwood (1990) was submitted to experimental verification (Romero and Davis, 1991), and it was able to quantitatively predict the effects of changes in the operating parameters. However, the predicted average permeation flux in steady state showed 50% deviations from the experimental ones.

The apparently good results obtained by Zydney and Colton (1986), which assumed blood as a constant viscosity fluid and made use of a linear velocity profile in the boundary layer, had already been discussed by Davis and Leighton (1987): the higher than real shear rates used would have balanced the lower predictions of diffusivity by the use of the correlation of Eckstein et al. These authors also studied the possibility that red blood cells have lower displacements induced by shear than do rigid spheres of comparable size, since they can deform and move one another.

The small bacteria used in this work, which are more resistant to deformation than red blood cells, make Eq. 8 bet-

ter suited to describe their diffusivity. It should also be noted that a compensation for shear rate values higher than reality did not take place. Therefore, to describe the experimental flux values by this model, the iterated cell volume fractions at the membrane surface (Table 4) became lower than the real ones. However, it was verified that the wall concentration was not very sensitive to shear rate values: if 40% lower shear rate values were used instead of those based on the bulk flow viscosity, only 14–18% higher wall concentrations would be obtained. The highest cell volume fraction at the membrane surface would be $\phi_m = 0.40$ instead of $\phi_m = 0.35$, which is still much lower than the maximum random packing volume fraction ($\phi_{max} \approx 0.6$–0.7). In a sheared suspension of rigid and inert 46-μm spheres ϕ_{max} was 0.58 (Leighton and Acrivos, 1987b); a layer of deformable red blood cells with $\phi_{max} = 0.90$ was assumed to be the cell concentration at the membrane surface in TFF of blood (Zydney and Colton, 1986). The excellent mixing promoted by the Taylor vortices was probably responsible for this low cell concentration at the membrane surface, which was only 2.5 times the bulk value at the higher concentration studied. Although making them depend on the estimation of cell concentration at the membrane surface, using Eq. 11 for flux predictions is much simpler and not more inaccurate than the model developed by Davis and collaborators.

These observations support the simplification of the constant shear rate made in this article. Therefore, the use of Eq. 11 for the calculation of the permeation flux in microfiltration, at the pressure-independent region of flux, is valid when vortex flow filtration is used.

Notation

b = coefficient of linear concentration term in a power law of D/D^0 (L/g)
C = solute concentration (g/L)
C_b = solute concentration in bulk flow (g/L)
C_f = solute concentration in the permeate (g/L)
C_l = layer solute concentration (g/L)
d = annular gapwidth (m)
d_h = hydraulic diameter (m), $d_h = 2d$
D = diffusion coefficient of the solute or shear-induced diffusion coefficient of cells (m^2/s)
D_b = diffusion coefficient computed for the bulk flow conditions (m^2/s)
D^0 = diffusion coefficient of the solute, at infinite dilution (m^2/s)
f = function
J = permeation flux ($m^3/m^2/s$, except as otherwise stated)
k_1 = mass-transfer coefficient in the pressure-dependent region of flux ($m^2 \cdot s/kg$)
$k_{II(I)}$ = mass-transfer coefficient in the pressure-independent region of flux (m/s)
k_m = mass-transfer coefficient in the membrane ($m^2 \cdot s/kg$)
ΔP = average transmembrane pressure (Pa, except as otherwise stated)
r_p = particle radius (m)
R = radius of the membrane–inner cylinder (m)
Re_a = axial Reynolds number, $Re_a = vd_h/\nu$
Re_t = tangential Reynolds number, $Re_t = \omega R d_h/\nu$
Sc = Schmidt number, $Sc = \nu/D$
Sh = Sherwood number, $Sh = k_1(d_h/D)(\Delta P - \Delta\pi)$ or $Sh = k_{II} d_h/D$
Ta = Taylor number, $Ta = \omega R d/\nu[d/(R + d/2)]^{1/2}$
v = axial fluid velocity (m/s)
x = linear coordinate, normal to membrane surface (m)

Greek letters

δ = boundary layer thickness (m)
ϕ = volume fraction of solute or particle
γ_m = shear rate at the membrane surface (s^{-1})
ω = angular velocity (rad/s)
ν = kinematic viscosity (m^2/s)
$\Delta\pi$ = osmotic pressure (Pa, except as otherwise stated)
ρ = fluid specific gravity (kg/m^3)
σ = solute rejection coefficient, $\sigma = (C_b - C_f)/C_b$

Literature Cited

Anderson, J. L., and C. C. Reed, "Diffusion of Spherical Macromolecules at Finite Concentration," *J. Chem. Phys.*, **64**, 3240 (1976).
Davis, R. H., and D. T. Leighton, "Shear-Induced Transport of a Particle Layer Along a Porous Wall," *Chem. Eng. Sci.*, **42**, 275 (1987).
Davis, R. H., and J. D. Sherwood, "A Similarity Solution for Steady-State Crossflow Microfiltration," *Chem. Eng. Sci.*, **45**, 3203 (1990).
Eckstein, E. C., D. G. Bailey, and A. H. Shapiro, "Self-Diffusion of Particles in Shear Flow of a Suspension," *J. Fluid Mech.*, **79**, 191 (1977).
Fair, B. D., D. Y. Chao, and A. M. Jamesion, "Mutual Translational Diffusion Coefficients in Bovine Serum Albumin Solutions, Measured by Quasielastic Laser Light Scattering," *J. Colloid Interf. Sci.*, **66**, 323 (1978).
Freifelder, D., *Physical Biochemistry — Applications to Biochemistry and Molecular Biology*, 2nd ed., W. H. Freeman, New York (1982).
Hinz, H.-J., *Thermodynamic Data for Biochemistry and Biotechnology*, Springer-Verlag, Berlin, p. 289 (1986).
Holeschovsky, U. B., and C. L. Cooney, "Quantitative Description of Ultrafiltration in a Rotating Filtration Device," *AIChE J.*, **37**, 1219 (1991).
Kataoka, K., H. Doi, and T. Komai, "Heat/Mass Transfer in Taylor Vortex Flow with Constant Axial Flow Rates," *Int. J. Heat Mass Transfer*, **20**, 57 (1977).
Kirkwood, J. G., and J. B. Shumaker, "Forces Between Protein Molecules in Solution Arising from Fluctuations in Proton Charge and Configuration," *Proc. Nat. Acad. Sci. U.S.A*, **38**, 863 (1952).
Leighton, D., and A. Acrivos, "Viscous Resuspension," *Chem. Eng. Sci.*, **41**, 1377 (1986).
Leighton, D., and A. Acrivos, "Measurement of Shear-Induced Self-Diffusion in Concentrated Suspensions of Spheres," *J. Fluid Mech.*, **177**, 109 (1987a).
Leighton, D., and A. Acrivos, "The Shear-Induced Migration of Particles in Concentrated Suspensions," *J. Fluid Mech.*, **181**, 415 (1987b).
Lojkine, M. H., R. W. Field, and J. A. Howell, "Crossflow Microfiltration of Cell Suspensions: A Review of Models with Emphasis on Particle Size Effects," *Trans. Inst. Chem. Eng.*, **70**, 149 (1992).
López-Leiva, M., "Ultrafiltration in a Taylor Vortex Flow," *AIChE Meeting*, Boston (Aug. 19, 1979).
Mateus, M., and J. M. S. Cabral, "Recovery of 6-α-Methylprednisolone from Biotransformation Medium by Tangential Flow Filtration," *Bioprocess Eng.*, **4**, 169 (1989).
Mateus, M., and J. M. S. Cabral, "Pressure-Driven Membrane Processes for Steroid Bioseparation: A Comparison of Membrane, Hydrodynamic and Operating Aspects," *Biosep.*, **2**, 279 (1991).
Mateus, M., J. A. L. Santos, and J. M. S. Cabral, "Membrane Separation Processes," *Recovery Processes for Biological Materials*, J. F. Kennedy and J. M. S. Cabral, eds., Wiley, West Sussex (1993).
Michaels, A. S., "New Separation Technique for the Chemical Process Industries," *Chem. Eng. Prog.*, **64**(12), 31 (1968).
Moore, W. J., *Physical Chemistry*, 4th ed., Prentice-Hall, London (1962).
Rolchigo, P. M., W. A. Raymond, and J. R. Hildebrand, "Improved Control of Ultrafiltration Using Vorticular Hydrodynamics and Hydrophilic Membranes," *Process Biochem.*, **24**, suppl. to 2, iii (1989).
Romero, C. A., and R. H. Davis, "Global Model of Crossflow Microfiltration Based on Hydrodynamic Particle Diffusion," *J. Memb. Sci.*, **39**, 157 (1988).
Romero, C. A., and R. H. Davis, "Experimental Verification of the

Shear-Induced Hydrodynamic Diffusion Model of Crossflow Microfiltration," *J. Memb. Sci.*, **62**, 249 (1991).
Vilker, V. L., C. K. Colton, K. A. Smith, and D. L. Green, "The Osmotic Pressure of Concentrated Protein and Lipoprotein Solutions and its Significance to Ultrafiltration," *J. Memb. Sci.*, **20**, 63 (1984).
Zydney, A. L., and C. K. Colton, "A Concentration Polarization Model for the Filtrate Flux in Cross-Flow Microfiltration of Particulate Suspensions," *Chem. Eng. Commun.*, **47**, 1 (1986).

Manuscript received Aug. 13, 1993, and revision received Apr. 25, 1994.